Inelastic neutron scattering study of the spin dynamics in Fe_3Si above T_C

L. Pintschovius
Kernforschungszentrum Karlsruhe G.m.b.H., Institut für Nukleare Festkörperphysik, Postfach 3640, D-7500 Karlsruhe 1, Federal Republic of Germany
(Received 20 August 1986)

High-resolution inelastic neutron scattering experiments have been performed on Fe_3Si at $T=1.12T_C$ using unpolarized neutrons. Special effort was made to isolate the magnetic contribution to the scattering intensity. For the whole range of momentum transfer $0.08\ \text{Å}^{-1} \lesssim q \lesssim 0.6\ \text{Å}^{-1}$, for which this separation was feasible, no indication was found for propagating modes. Instead, $S(q,\omega)$ can be well described by a double-Lorentzian scattering function typical for spin-diffusion behavior. In particular, the maximum of the scattering intensity always occurs at zero energy transfer. A closer look at the scattering function reveals that it gradually changes from a truncated Lorentzian at small q to a more Gaussian form at large q. As a consequence, our results agree with the predictions of the dynamic scaling theory only in that area of (q,ω) space which lies below the spin-wave dispersion curve for $T \lesssim T_C$.

I. INTRODUCTION

The nature of the paramagnetic phase of itinerant ferromagnets has been a subject of considerable controversy in the last years. The fluctuating-band theory[1-3] is based upon the existence of very strong short-range magnetic order (SRMO). Because of the itineracy of the d electrons, the strong SRMO is assumed to exist not only in the vicinity of the phase transition, but well above T_C. The typical extension of SRMO was estimated to be 20 Å, if the spin-spin correlation function is averaged over times of the order 10^{-13}–10^{-14} s. Other theories[4-8] describe the paramagnetic phase as having no appreciable SRMO outside the critical region. Experimental evidence to decide between the two lines can be obtained by inelastic neutron scattering: In the absence of SRMO a magnetic scattering function of the spin diffusion type is expected throughout the Brillouin zone:

$$S(q,\omega) \sim \frac{\Gamma}{\Gamma^2+\omega^2} . \tag{1}$$

On the other hand, propagating spin waves should be observable at short wavelengths also above T_C if a strong SRMO persists.

The observation of propagating spin waves above T_C has indeed been reported by Mook *et al.*,[9] Lynn,[10] and Lynn and Mook[11] for Fe and Ni. Later on, their interpretation of the data has been contested by Shirane and coworkers.[12-18] They carried out a series of polarized neutron scattering experiments, again on the paramagnetic phases of Fe and Ni.[12-18] A scattering function of Lorentzian type both in energy and momentum transfer was shown to describe the cross sections quantitatively. The spin-wave-like excitations in Ni above T_C were explained by Uemura *et al.*[19] to be nothing but constant-E cuts through the paramagnetic scattering function. On the other hand, Lynn and Mook resumed their experiments using also the polarized-neutron technique. Although the results of the new experiments differ noticeably from their previous findings, they still claim that spin-diffusion behavior is only observed at small q, but that at larger q the magnetic response peaks at finite energies.[20,21] A strong SRMO has been advocated by Ziebeck *et al.*[22] and Brown *et al.*[23-25] on the basis of different experiments. They investigated which values of q contribute significantly to the Fourier spectrum of the spin-density–spin-density correlation function. For that purpose the quasielastic magnetic response was measured with an intentionally low energy resolution to get directly the energy-integrated magnetic intensity $I(q)$. They plotted $I(q)q^2$ versus q (the factor q^2 is a phase space factor) and obtained a peak at $q \approx 0.35\ \text{Å}^{-1}$ for Fe at $T=1.25T_C$. From the position of this peak intensity they deduced a ferromagnetic correlation length of 15–20 Å. This conclusion has been disputed by Edwards[26] for two reasons. Firstly, because he thinks that the data have to be analyzed in a different way, and secondly, because he presumes that the measured intensities at large q are considerably too small.

As it has turned out that all evidence supporting a strong SRMO above T_C is questionable, we considered it desirable to perform further experimental investigations which might help to clarify the situation. For that reason we continued earlier neutron scattering measurements by Blanckenhagen *et al.*[27,28] on Fe_3Si, a compound which can be regarded as a close relative to bcc Fe. The previous results looked similar to those of Lynn and Mook, i.e., they seemed to indicate the persistence of spin waves far above T_C. However, after extending the measurements to a much wider area of (q,ω) space than before, we realized that the interpretation of the previous data had to be revised. In this paper we present the results of a new series of inelastic neutron scattering experiments aiming at a determination of the magnetic response at $T=1.12T_C$. The data are analyzed by a double-Lorentzian scattering function as proposed by dynamic scaling theory. The shortcomings of this type of analysis are discussed. It is checked how far these shortcomings can be overcome by

using the shape function recently proposed by Folk and Iro.[29] Further, we looked for a peak in the curve $I(Q)Q^2$ versus Q as suggested by Brown *et al.*[24] and Capellmann.[2]

II. EXPERIMENTAL TECHNIQUE

The sample was the same as had been used in our previous investigations:[27,28] A single crystal of about 3 cm^3 volume showing a mosaic spread of 0.4°. The Curie temperature T_C was deduced from the temperature dependence of the (111) Bragg intensity to lie at $T_C = 830$ K. During the neutron scattering experiments the temperature of the sample was stabilized to about ± 2 K.

The measurements were performed on the 1T and 2T triple-axis spectrometers at the 14-MW medium flux ORPHEE reactor in Saclay. A preliminary data set was obtained with pyrolitic graphite (PG) (002) as monochromator and analyzer and a collimation of 50'-35'-30'-20'. The incident energy was chosen around 14 meV and a PG filter was used to remove higher order contaminations. Most scans were made in the neutron energy gain mode. The energy resolution was $\Delta E = 0.8$ meV [full width at half maximum (FWHM)], increasing to $\Delta E = 2.3$ meV at $E = -35$ meV. The most complete data set was taken with Cu(220) as monochromator and analyzer and a collimation of 50'-35'-30'-30'. In this case the incident energy was chosen around 35 meV and the energy transfer investigated ranged between $7 > E > -46$ meV. Again most scans were made in the neutron-energy-gain mode. The energy resolution varied between $\Delta E = 0.9$ meV ($E = 7$ meV) and $\Delta E = 3$ meV ($E = -46$ meV). Additional measurements for small values of q and $\hbar\omega$ were performed with Ge(111) and PG(002) as monochromator and analyzer, respectively, and a collimation of 50'-40'-40'-50'. The lowest incident energy used was $E_0 = 6.2$ meV, resulting in an energy resolution of $\Delta E = 0.3$ meV. In this case a PG filter was employed to suppress the third order (the second and fourth order being absent). As the different instrumental configurations were used in overlapping q ranges, we were able to normalize all intensities to that of our standard configuration.

The neutron-energy-gain mode of operation has the advantage that for sample temperatures much higher than the reactor moderator temperature the scattering intensity is higher than for the corresponding instrumental configuration in the neutron energy-loss mode. However, it has also a serious drawback: In order to obtain a reasonable variation of the instrumental resolution, high resolution at zero energy transfer and relaxed resolution at large energy transfers, the scans have to be made in the constant-k_i mode. In this type of scan the spectrometer efficiency strongly varies with the outgoing energy. Although the correction of the measured intensities for this variation is in principle simple,[30] in practice it is somewhat troublesome because it requires an accurate knowledge of the energy dependence of the analyzer reflectivity R_A and the detector efficiency η_D. To get these data, preparatory experiments have been performed yielding the product $R_A\eta_D$ for the whole range of final energies used in the later scans.

The spectrometers used did not allow a polarization analysis. As is well known, unpolarized neutron scattering techniques give much higher intensities than polarized-beam techniques, thus allowing for a considerably better resolution. On the other hand, using unpolarized neutrons it is difficult to isolate the magnetic contribution to the scattering intensity from other sources, like phonon, multiphonon, incoherent nuclear, empty can, and general instrumental background scattering. The separation is particularly difficult when the magnetic response is smeared out over a large area in (q,ω) space, as had to be expected in our case. To overcome this problem, a large number of reference scans were made at temperatures below T_C. Such scans should be made as close to the temperature of interest as possible to reduce the uncertainty arising from the temperature dependence of the nonmagnetic scattering. However, approaching T_C results in a broadening of the magnetic excitations which complicates the separation of magnetic and nonmagnetic contributions already in this temperature regime. As a compromise, a maximum temperature $T = T_C - 90$ K $= 740$ K was chosen for reference scans, which is 190 K below the temperature at which the paramagnetic scattering was investigated. Since the temperature dependence of the nuclear scattering intensity cannot be neglected for such a wide temperature interval, additional reference scans were made at room temperature and at $T = 530$ K, aiming at a reliable extrapolation to $T = T_C + 100$ K. Measurements at many different points in (q,ω) space revealed that the temperature dependence of the nonmagnetic scattering was essentially linear. A linear extrapolation of the nonmagnetic scattering intensities from temperatures below T_C to $T = T_C + 100$ K was confirmed for those values of q and ω where the magnetic scattering intensity was likely to be very small also above T_C (see Fig. 1). Therefore the extrapolation procedure was used throughout the whole area of (q,ω) space covered by our

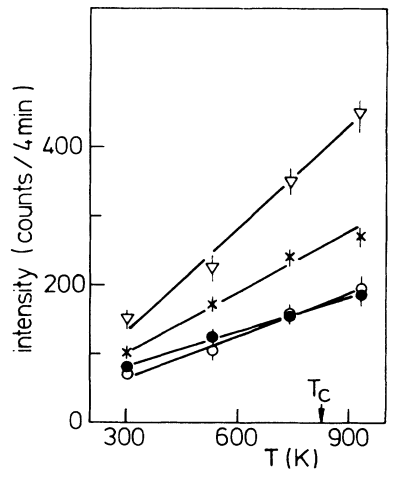

FIG. 1. Nonmagnetic scattering intensity versus temperature for selected points in (q,ω) space. All data shown in this figure have been collected in those areas in (q,ω) space where the magnetic scattering is expected to be very small in the whole temperature range.

measurements. We think that in this way the problem of background correction is solved as completely as possible for scattering of unpolarized neutrons. Of course, the solution is not perfect: Statistical errors and possible departures of the temperature dependence of the background intensity from a linear behavior produce uncertainties which limit the sensitivity and accuracy of this method. This is particularly true for those values of q and ω where the one-phonon cross section is large. Here the background correction cannot be made reliably, which means that some "blind spots" are inherent to the method.

The data were collected in the vicinity of the (1,1,1) reciprocal-lattice point, because it has the smallest Q value ($Q=1.93$ Å^{-1}) and in addition a low structure factor for long-wavelength phonons.

III. RESULTS AND ANALYSIS

Fe_3Si crystallizes in the DO_3-type structure, which can be described as four interpenetrating fcc lattices: one of Si, one of Fe(1), and two of Fe(2). This phase is stable up to temperatures far above T_C. From the lattice constant $a_0=5.655$ Å the distance between nearest Fe neighbors is inferred to be $d=1.632$ Å, which is close to the corresponding value in bcc Fe ($d=1.655$ Å). As the primitive unit cell contains four atoms there are 12 phonon branches for every direction. In order to know where in (q,ω) space to expect intense neutron groups due to one-phonon scattering, a survey investigation of the lattice dynamics of Fe_3Si was carried out at $T=930$ K. The data were fitted to a 13 parameter Born–von Kármán model. Inelastic structure factors computed from this model were used to search for those areas in (q,ω) space which are best suited for the investigation of the magnetic scattering. It turned out that Q parallel to [111] was generally the best choice. Here only the four branches with Λ_1 symmetry have a non-zero structure factor. These branches are shown in Fig. 2.

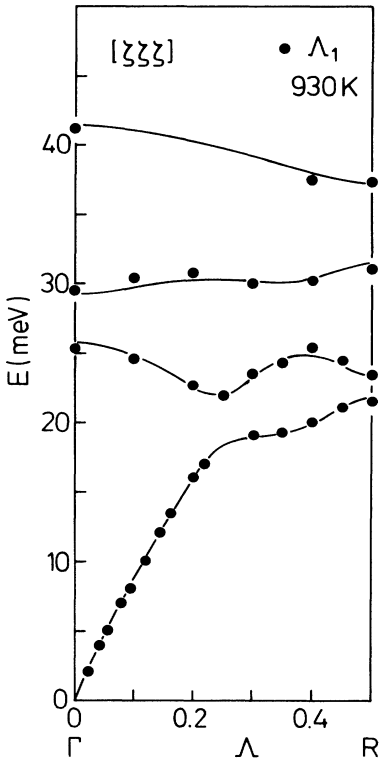

FIG. 2. Phonon-dispersion curves of Fe_3Si in the [111] direction at $T=930$ K. Only the branches with Λ_1 symmetry ("longitudinal" branches) are shown. The lines have been calculated on the basis of a 13-parameter Born–von Kármán model fitted to the experimental data.

The scans aiming at a determination of the magnetic scattering at $T=1.12T_C$ were carried out as a series of constant-E scans. As has been observed in the case of Ni and Fe,[9–11,14] such scans yield well defined magnetic peaks also at $T>T_C$. Figure 3 shows an example for a relatively high energy transfer, i.e., $E=-35.5$ meV. For comparison the corresponding scan at $T=0.9T_C$ is given too. The shift in peak position between $T=0.9T_C$ and $T=1.12T_C$ is relatively large when compared to the corresponding shift in Fe,[9] which can be traced back to a stronger temperature dependence of the stiffness constant in Fe_3Si for temperatures approaching T_C.

As has been shown by Uemura *et al.*,[19] well-defined peaks in constant-E scans cannot be taken as evidence for the possibility of propagating spin waves above T_C. Instead, conclusions about the persistence of spin-wave-like excitations can only be drawn from constant-q scans. Therefore we have evaluated constant-q scans from our data after subtracting the nonmagnetic scattering as described in Sec. II. Some examples of such scans are given in Fig. 4. The data resemble those which have been reported in Refs. 12–16 for the paramagnetic scattering of Ni and Fe–4 at.% Si: The maximum intensity is always found at $E\approx 0$ and the linewidth is rapidly increasing with q. It is known that such a behavior of the scattering function is predicted by dynamical scaling theory[31] for spin fluctuations. The data in Refs. 12–18 can be described quantitatively by this theory. We therefore tried to analyze our data in the same way. The scattering function is assumed to be given by

$$S(q,\omega)=S_0\frac{\kappa^2}{\kappa^2+q^2}\frac{\Gamma}{\Gamma^2+\omega^2}\frac{\hbar\omega/kT}{1-\exp(-\hbar\omega/kT)}\ , \tag{2}$$

where S_0 is a constant, $\kappa=\kappa(T)$ an inverse correlation length and Γ is the energy width. Résibois and Piette[32] have found that

$$\Gamma=Af(\kappa/q)q^{5/2}\ , \tag{3}$$

where A denotes a constant and the scaling function $f(\kappa/q)$ has the asymptotic behavior.

$$f(\kappa/q)\rightarrow\begin{cases}1 & \text{when } \kappa/q\rightarrow 0\ ,\\ (\kappa/q)^{1/2} & \text{when } \kappa/q\rightarrow\infty\ .\end{cases} \tag{4}$$

Following the procedures of Uemura *et al.*,[19] we have assumed that the scaling function has the simple form

$$f(\kappa/q)=\begin{cases}1 & \text{when } q\geq\kappa\ ,\\ (\kappa/q)^{1/2} & \text{when } q<\kappa\ .\end{cases} \tag{5}$$

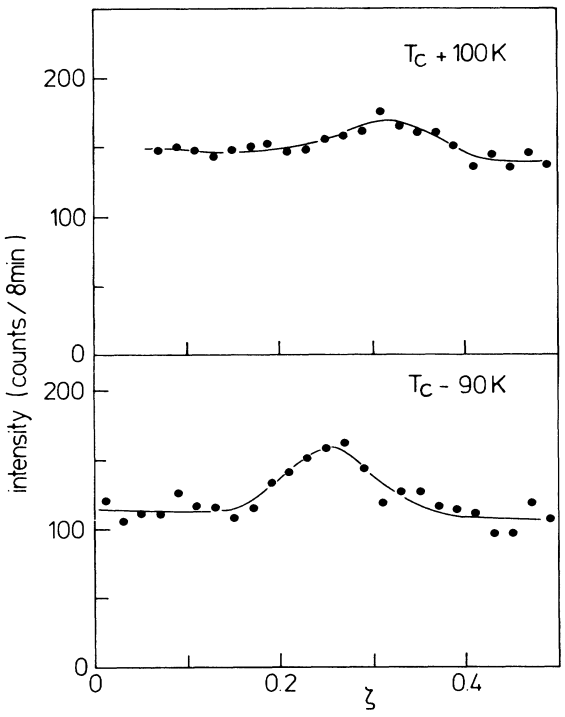

FIG. 3. Constant-E scans for $E=-35.5$ meV at $T=T_C-90$ K (below) and $T=T_C+100$ K (above) for $Q=(1+\zeta, 1+\zeta, 1+\zeta)$. Lines are a guide to the eye. The data are the average of several runs.

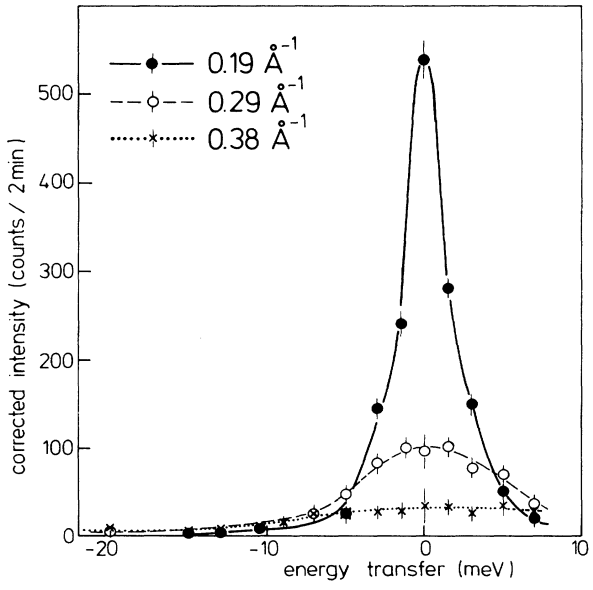

FIG. 4. Three constant-q scans at $T=930$ K deduced from a series of constant-E scans. The background has been subtracted. The intensities have been corrected for the spectrometer efficiency. Lines are a guide to the eye.

The scattering function can be deduced from the magnetic scattering cross section by use of the relation

$$\frac{d^2\sigma}{d\omega\, d\Omega} \sim f^2(q+\tau)e^{-2W}S(q,\omega)\ , \tag{6}$$

where f^2 denotes the magnetic form factor, τ the reciprocal-lattice vector and e^{-2W} the Debye-Waller factor. For the form factor we have used the values of Weiss and Freeman for Fe,[33] and the Debye-Waller factor has been estimated from the lattice dynamical properties. After correcting for f^2 and e^{-2W} the constant-q scans for $\tau+q$ and $\tau-q$ have been combined on common plots and from these plots we have evaluated the intensity I_0 at $E=0$ and the linewidth Γ. In order to determine S_0, κ, and A we have plotted I_0 and Γ versus q on a log-log scale in Figs. 5 and 6. Evidently, the data can be well described by curves computed from Eqs. (2), (3), and (5). We note that the observed energy widths and intensities cover two and three orders of magnitude, respectively. The fit yielded the values $\kappa=0.16$ Å^{-1} and $A=142$ meV Å$^{5/2}$, which are similar to the corresponding values in Fe–4 at.% Si at $T=1.12T_C$, reported by Wicksted *et al.*,[15] i.e., $\kappa=0.23$ Å^{-1} and $A=142.3$ meV Å$^{5/2}$.

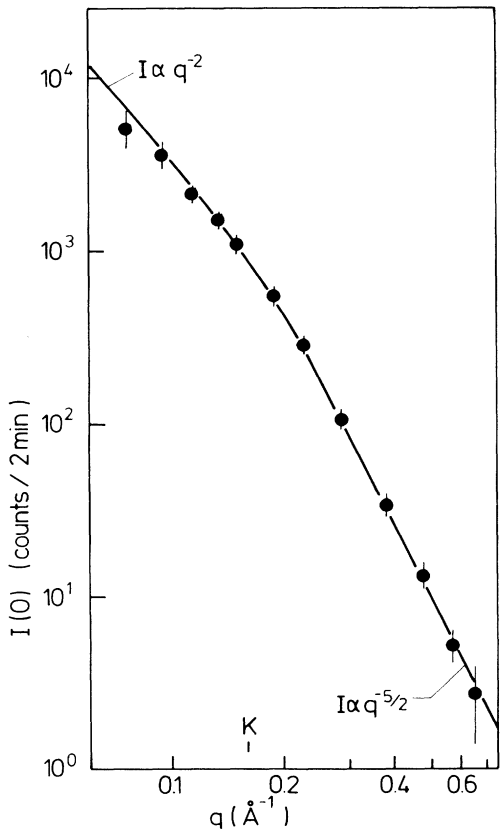

FIG. 5. Magnetic intensities at $E=0$ versus q for $T=930$ K. The intensity values have been corrected for the magnetic form factor. Data obtained with different instrumental parameters have been normalized to the values around $q=0.2$ Å^{-1}. The line is the result of a fit based on a scattering function described by Eqs. (2) and (3).

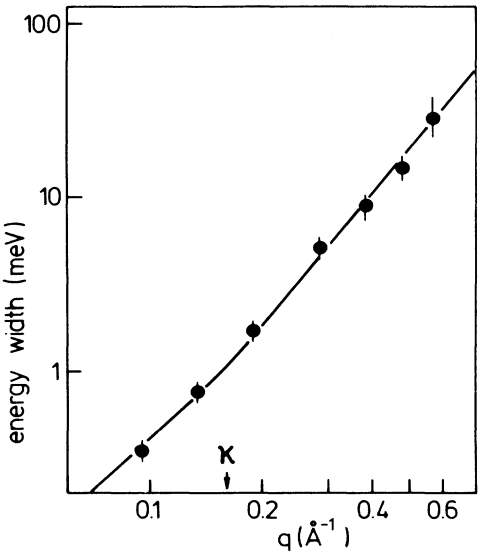

FIG. 6. Observed energy width (FWHM) versus q at $T=930$ K for the magnetic scattering. The line is the result of a fit based on Eq. (3).

For detailed comparison, Figs. 7(a)—7(f) show the calculated scattering function and the observed intensities for six q values in the range $0.096 \leq q \leq 0.58$ Å^{-1}. Note the different scales both for intensities and energies. The calculated curves have not been convoluted with the resolution function as the instrumental resolution was in all cases much smaller than the observed energy width. Clearly, the agreement between calculated and experimental intensities is very satisfactory. For $q \geq 0.48$ Å^{-1} the scatter of the data is rather large, mainly because of the uncertainties of the background subtraction. Nevertheless, there is clear evidence that the scattering function is always centered around $E=0$, which means that the data do not show a crossover from spin-diffusive behavior to propagating behavior within the range $q \lesssim 0.6$ Å^{-1}. Admittedly, a theory giving a strong Lorentzian line centered around zero and two weak Lorentzian lines around $\pm\hbar\omega$ may not be incompatible with the data. A much higher precision would be necessary to discriminate this case from a single broad line around zero.

Although calculated and observed intensities agree generally quite well, there are systematic deviations for energies $E > \Gamma$. Here the scatter of the data is comparatively small because of a better signal-to-noise ratio than for energies around zero, which allows a detailed comparison despite the low intensity levels. It appears that the observed intensities decrease more rapidly with increasing energy transfer than predicted. For $\zeta=0.05$ $[Q=(1+\zeta, 1+\zeta, 1+\zeta)]$ this effect is very small up to $E/\Gamma \approx 3$, but even here the experimental intensities fall below the calculated values when going further out (see Fig. 8). For larger ζ values the deviations between theory and experiment become more pronounced, so the observed scattering function gradually takes on a more Gaussian form.

The agreement between theory and experiment can be checked in a more direct way by calculating intensities for constant-E scans. The examples given in Figs. 9 and 10 are representative in the sense that there is very good agreement between calculated and observed intensities for small energy transfers, but that considerable deviations occur at large energy transfers and small q. This is just another illustration of the fact that the scattering function is not adequately described by a Lorentzian for $E/\Gamma \gg 1$.

Figures 9(a)—9(d) illustrate the problem of evaluating the paramagnetic scattering in a wide area of (q,ω) space by means of unpolarized neutron scattering. For $E=1.5$ meV the scattering intensity falls off very rapidly with increasing q. At first glance the background level seems to be reached at $\zeta \approx \pm 0.3$. Only after expanding the intensity scale (requiring better counting statistics) it becomes evident that the background level is not reached before $\zeta \approx 0.4$. The magnetic scattering intensity at $\zeta \pm 0.3$ may appear to be fairly small. Nevertheless it is not small when compared to the corresponding intensity for large energy transfers. To demonstrate this, the constant-E scan at $E=-35.5$ meV has been plotted in Figs. 9(c) and 9(d) on the same scales as used for the scan at $E=1.5$ meV. Obviously, the determination of constant-q scans for large q values required careful studies of the intensity distributions at small energy transfers and in particular painstaking estimates of the background.

Our results are summarized in Figs. 11(a) and 11(b), where contour maps are shown for a double Lorentzian and the experimentally determined scattering function. The inadequacy of a Lorentzian shape function for $E/\Gamma \gg 1$ has been found already by Lynn and Mook[11] for Ni and by Wicksted *et al.*[15] for Fe. Wicksted *et al.* modified the Lorentzian shape function in a heuristic way to get a better agreement with experiment. Recently, Folk and Iro[29] have used the asymptotic renormalization-group theory to obtain a better-founded modification of the shape function. In order to test their predictions, we have calculated the width Δq of the peak in constant-E scans with their shape function and compared to experiment (see Fig. 12). Obviously, the shape function proposed by Folk and Iro gives a somewhat better agreement with experiment than a Lorentzian, but the agreement is still not satisfactory. We think a major drawback of this theory lies in the fact that it still yields a universal shape function, whereas the experiment shows that the shape function is q dependent. Perhaps a hint for a better understanding of the shape functions can be obtained from the following observation: The experimental shape function starts to fall below the Lorentzian at about that energy $E(q)$ which corresponds to the magnon energy just below T_C. This means that the breakdown of long-range order at T_C redistributes $S(q,\omega)$ in such a way that spectral weight is pushed to lower frequencies, but barely to higher ones.

In Ref. 10 Lynn has plotted a constant-q scan measured on Fe—4 at.% Si [hereafter abbreviated as Fe(Si)] at $T=1.28T_C$, which shows a pronounced peak at $E=20$ meV. This peak was taken as strong evidence for the persistence of propagating spin waves above T_C. We have compared the lineshape of the scattering function reported for Fe(Si) to that observed in Fe_3Si at $T=1.12T_C$ for the

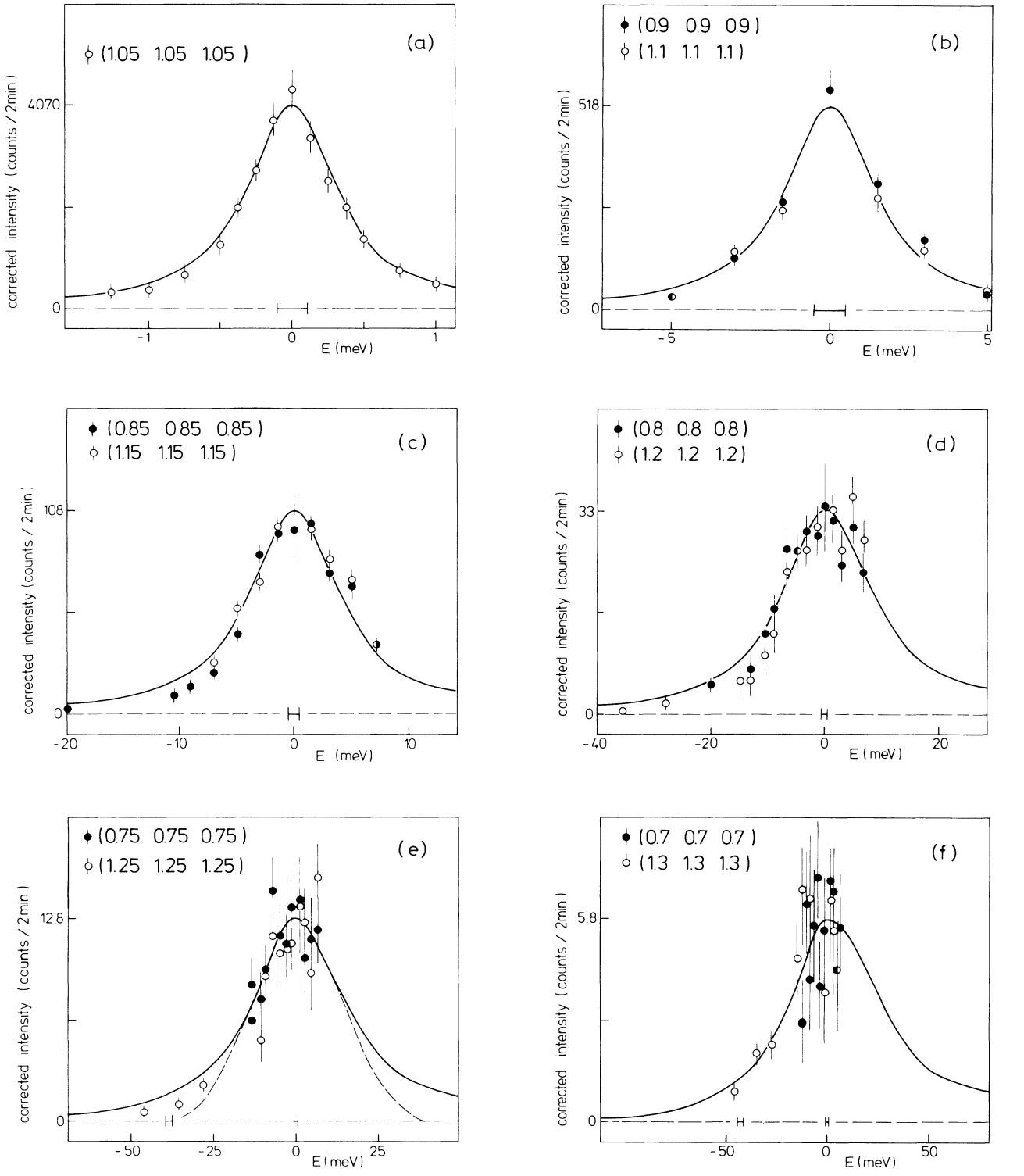

FIG. 7. Constant-q scans for six q values deduced from a series of constant-E scans at $T=920$ K. The background has been subtracted. The intensity values have been corrected for the spectrometer efficiency, the magnetic form factor and the Debye-Waller factor. All data were collected with $E_f=35$ meV, except those shown in Fig. 7(a) which were determined with $E_i=6.3$ meV and normalized accordingly. The solid lines have been calculated with the aid of Eqs. (2) and (3) after adjusting the parameters S_0, κ, and A. Note the different scales both for the intensity and the energy. For comparison, a Gaussian has also been plotted in Fig. 7(e). The horizontal bars indicate the instrumental energy resolution.

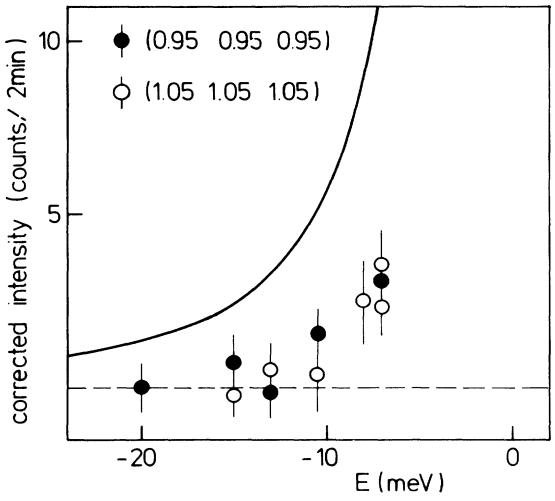

FIG. 8. High-energy tail of the shape function for $\zeta = \pm 0.05$ [see Fig. 7(a)]. The data were collected with $E_f = 35$ meV. The solid line has been calculated from Eqs. (2) and (3).

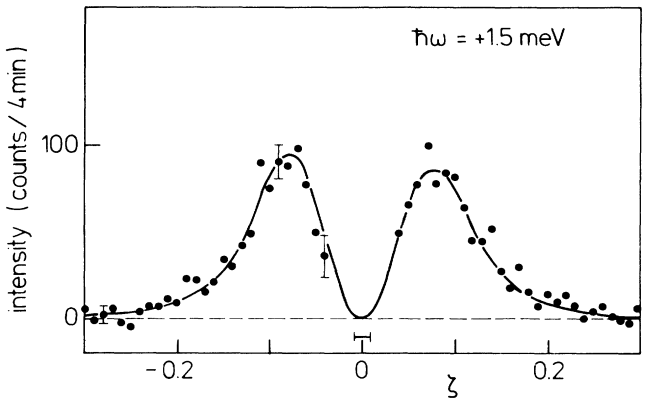

FIG. 10. Constant-E scan at $E = 1.5$ meV measured at $Q = (1+\zeta, 1+\zeta, 1+\zeta)$ with very high resolution ($E_i = 6.3$ meV). The nonmagnetic scattering has been subtracted. Some data points around $\zeta = 0$ have been omitted, because phonon peaks at $\zeta = \pm 0.02$ did not allow a reliable determination of the magnetic contribution in this region.

same wave vector ($q = 0.47$ Å^{-1}). We note that the shapes are very similar for energies $E > 20$ meV. The fact that Lynn reported a peak in the constant-q scan which is absent in our data can be traced back to strong differences in the low energy region. Here, the measurements are particularly delicate as has been explained above.

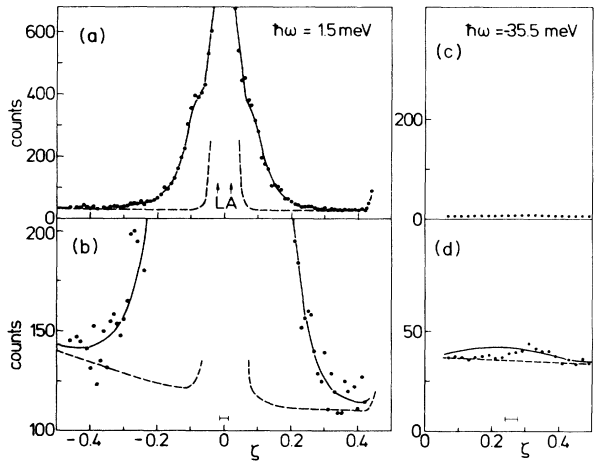

FIG. 9. Constant-E scans at $E = +1.5$ meV and $E = -35.5$ meV. The data were taken at $Q = (1+\zeta, 1+\zeta, 1+\zeta)$ with $E_f = 35$ meV. The intensities at $E = +1.5$ meV and $E = -35.5$ meV are normalized in respect to the spectrometer efficiency. In the lower plots the intensity scale has been expanded by a factor of 6 and the counting times increased by a factor of 4 when compared to the upper plots. The dashed lines show the estimated nonmagnetic scattering. The solid lines have been calculated from Eqs. (2) and (3). The horizontal bars denote the instrumental q resolution. The arrows show the position of the longitudinal acoustic (LA) phonon peaks.

In the end, we want to investigate whether there is a peak in the curve $I(q)q^2$ versus q. As has been pointed out in the Introduction the observation of such a peak in Fe has been interpreted by Brown *et al.*[24] and Capellmann[2] as evidence for a strong SRMO. The results of our analysis are plotted in Fig. 13. In a first step we have assumed that the shape function is Lorentzian in the whole q range investigated which yields the solid line in the figure. In a next step we have estimated the changes produced by the deviations from a Lorentzian shape function, which yielded the broken line. The broken line levels off earlier than the solid line, but does not show a real peak within the range of the data, whereas Brown *et al.*[24] have observed a clear peak at $q \approx 0.35$ Å in Fe(Si) at $T = 1.22 T_C$. Therefore following the lines of Brown *et al.* and Capellmann one has to conclude that any magnetic order in Fe_3Si above T_C must be of considerably shorter range than that deduced for Fe(Si), i.e., ≈ 15 Å. Finally we have simulated the experimental procedure of Brown *et al.* by calculating the q dependence of the magnetic scattering intensity using a spectrometer with an energy resolution of 50 meV (FWHM) operated in the $E = 0$ mode. This simulation yielded the dashed-dotted line in Fig. 13. Now there appears a distinct peak at $q \approx 0.35$ Å^{-1}, which coincides with the position of the corresponding peak in Fe(Si) mentioned above. Obviously, the peak for Fe_3Si is an artifact of the evaluation procedure and has no physical meaning. From the similarity of the magnetic properties of Fe(Si) and Fe_3Si we suspect the peak reported for Fe(Si) to have a trivial reason as well.

IV. CONCLUSIONS

By a detailed investigation of the nonmagnetic contributions to the scattering intensity it was possible to determine the paramagnetic scattering in Fe_3Si in a wide range of (q,ω) space by using unpolarized neutrons. For small

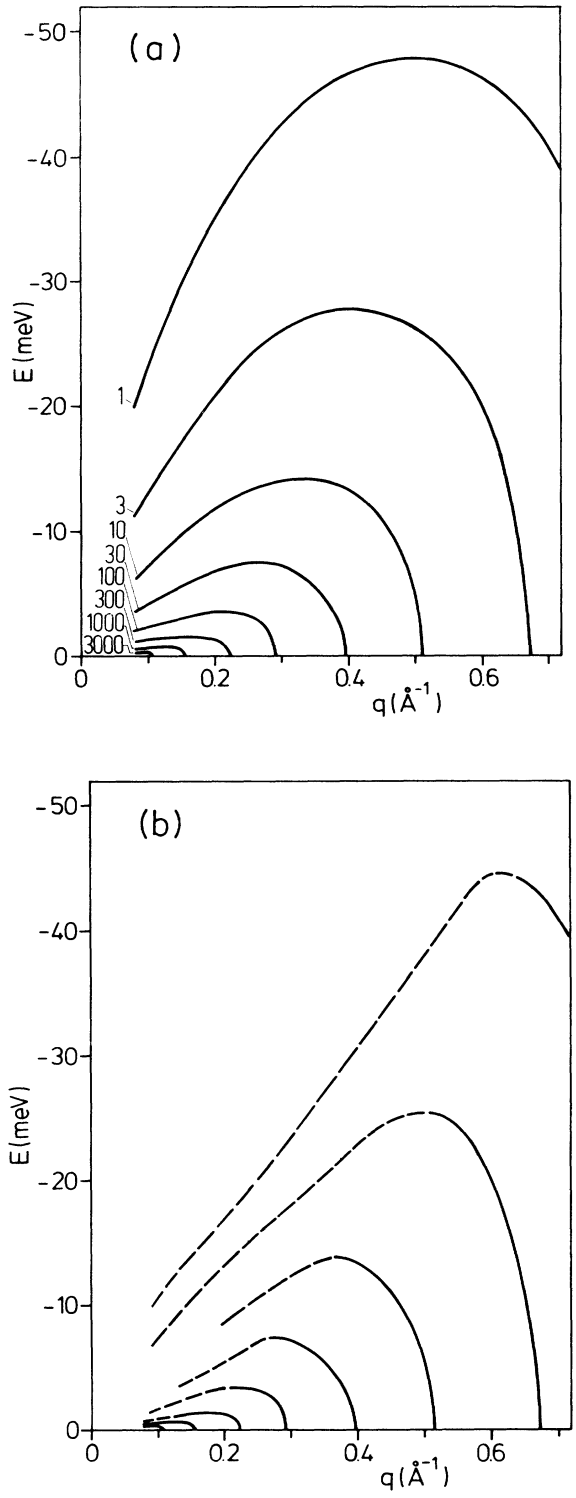

FIG. 11. Maps of constant intensity contours in (q,ω) space as calculated from (a) Eqs. (2) and (3) and as constructed from (b) constant-E scans close to the (1,1,1) reciprocal lattice point. In that region where the data can be very well described by Eqs. (2) and (3) the experimental contour lines have been plotted as solid lines. The remaining part of the experimental intensity contours has been plotted as dotted lines.

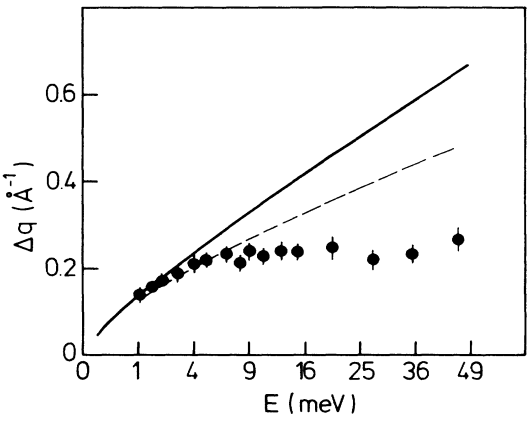

FIG. 12. Observed full width at half maximum (in q) for constant-E scans. The solid line shows the values calculated from Eqs. (2) and (3). The dashed line is obtained when the Lorentzian shape function in Eq. (2) is replaced by the shape function proposed by Folk and Iro (Ref. 23).

q, the results could be well described by a double-Lorentzian scattering function derived from dynamical scaling theory. At larger wave factors, there are noticeable deviations from a Lorentzian shape function, but no indication was found for a crossover from spin-diffusive behavior at small wave vectors to propagating behavior at larger wave vectors within the accessible range $q \lesssim 0.6$ Å^{-1}. Thus, our results do not indicate the occurrence of

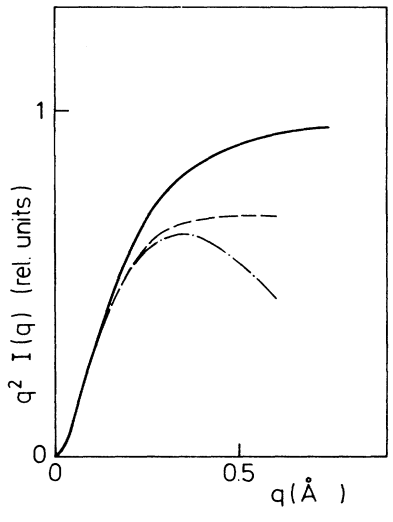

FIG. 13. $q^2I(q)$ as a function of q in Fe_3Si at $T=930$ K. The solid line has been calculated from Eqs. (2) and (3). The dashed line is obtained if the deviations of the observed shape functions from a Lorentzian are taken into account. The dashed-dotted line simulates a measurement using a spectrometer with a resolution of 50 meV (FWHM) operated in the $E=0$ mode.

a strong SRMO above T_C. Furthermore, the plot $I(q)q^2$ versus q did not show a peak, as had to be expected after Brown *et al.*[24] for a material with strong SRMO. Our results agree well with those of Refs. 12—18 in which the picture of giant short-range order above T_C advocated by other groups has been strongly contested. We cannot rule out spin correlations on a very short length scale: As our data do not give reliable evidence in the range $q > 0.6$ Å^{-1}, spin clusters may be present with diameters $d < 2\pi/0.6 \approx 10$ Å. Therefore the question, whether or not the "local band" theory of itinerant ferromagnets is justified for Fe_3Si, may be regarded as still not answered. However, we feel that such a theory based on the presence of ferromagnetic clusters of less than 10 Å diam is questionable, because in such small clusters more than 50% of the spins are sitting at the surface. In this sense we consider our results as evidence against the appropriateness of such theories.

ACKNOWLEDGMENTS

I would like to thank Dr. Peter von Blanckenhagen for technical help and a critical reading of the manuscript.

[1]V. Korenman, J. L. Murray and R. E. Prange, Phys. Rev. B **16**, 4032 (1977); **16**, 4048 (1977); **16**, 4058 (1977); R. E. Prange and V. Korenman, *ibid.* **19**, 4091 (1979); **19**, 4698 (1979); V. Korenman and R. E. Prange, Solid State Commun. **31**, 909 (1978).

[2]H. Capellmann, J. Phys. F **4**, 1466 (1974); Solid State Commun. **30**, 7 (1979); Z. Phys. B **35**, 269 (1979); J. Magn. Magn. Mater. **21**, 213 (1980); **28**, 250 (1982).

[3]J. B. Sokoloff, Phys. Rev. Lett. **31**, 1417 (1974).

[4]H. Hasegawa, J. Phys. Soc. Jpn. **46**, 1540 (1979); **49**, 178 (1980).

[5]B. S. Shastry, D. M. Edwards, and A. P. Young, J. Phys. C **14**, L665 (1981).

[6]T. Moriya, J. Magn. Magn. Mater. **14**, 1 (1979).

[7]J. Hubbard, Phys. Rev. B **19**, 2626 (1979); **20**, 4585 (1980).

[8]B. L. Gyorffy, A. J. Pindor, J. Staunton, G. M. Stocks, and H. Winter, J. Phys. F **15**, 1337 (1985).

[9]H. A. Mook, J. W. Lynn, and R. M. Nicklow, Phys. Rev. Lett. **30**, 556 (1973).

[10]J. W. Lynn, Phys. Rev. B **11**, 2624 (1975).

[11]J. W. Lynn and H. A. Mook, Phys. Rev. B **23**, 198 (1981).

[12]O. Steinsvoll, C. F. Majkrzak, G. Shirane, and J. Wicksted, Phys. Rev. Lett. **51**, 300 (1983).

[13]J. P. Wicksted, G. Shirane, and O. Steinsvoll, Phys. Rev. B **29**, 488 (1984).

[14]O. Steinsvoll, C. F. Majkrzak, G. Shirane, and J. Wicksted, Phys. Rev. B **30**, 2377 (1984).

[15]G. Shirane, O. Steinsvoll, Y. J. Uemura, and J. Wicksted, J. Appl. Phys. **55**, 1887 (1984); J. P. Wicksted, P. Böni, and G. Shirane, Phys. Rev. B **30**, 3655 (1984); G. Shirane, P. Böni, and J. P. Wicksted, Physica **127B**, 264 (1984).

[16]P. Böni and G. Shirane, J. Appl. Phys. **57**, 3012 (1985).

[17]J. L. Martinez, P. Böni, and G. Shirane, Phys. Rev. B **32**, 7037 (1985).

[18]G. Shirane, P. Böni, and J. P. Wicksted, Phys. Rev. B **33**, 1881 (1986).

[19]Y. J. Uemura, G. Shirane, O. Steinsvoll, and J. Wicksted, Phys. Rev. Lett. **51**, 2322 (1983).

[20]H. A. Mook and J. W. Lynn, J. Appl. Phys. **57**, 3006 (1985).

[21]J. W. Lynn and H. A. Mook, J. Magn. Magn. Mater. **54-57**, 1169 (1986).

[22]K. R. A. Ziebeck, P. J. Brown, J. G. Booth, and J. A. C. Bland, J. Phys. F **11**, L127 (1981).

[23]P. J. Brown, J. Déportes, D. Givord, and K. R. A. Ziebeck, J. Appl. Phys. **53**, 1973 (1982).

[24]P. J. Brown, H. Capellmann, J. Déportes, D. Givord, and K. R. A. Ziebeck, J. Magn. Magn. Mater. **30**, 243 (982).

[25]P. J. Brown, K. R. A. Ziebeck, J. Déportes, and D. Givord, J. Appl. Phys. **55**, 1881 (1984).

[26]D. M. Edwards, J. Magn. Magn. Mater. **36**, 213 (1983).

[27]P. v. Blanckenhagen and C. Lin, in *Physics of Transition Metals,* edited by P. Rhodes (IOP, Bristol, 1981), p. 371.

[28]P. v. Blanckenhagen and C. Lin, Physica **120B**, 173 (1983).

[29]R. Folk and H. Iro, Phys. Rev. B **32**, 1880 (1985).

[30]B. Dorner, Acta Crystrallogr. Sect. A **28**, 319 (1972).

[31]B. I. Halperin and P. C. Hohenberg, Phys. Rev. **177**, 952 (1969).

[32]R. Résibois and C. Piette, Phys. Rev. Lett. **24**, 514 (1970).

[33]R. J. Weiss and A. J. Freeman, J. Phys. Chem. Solids **10**, 147 (1959).